Top Catal (2010) 53:403–416
DOI 10.1007/s11244-010-9453-4

ORIGINAL PAPER

Symmetric Transition State Analysis: An Analysis of Dissociative Methane Adsorption on Rh{111} Using Quantum Chemical Calculations

Bouke S. Bunnik · Gert-Jan Kramer · Rutger van Santen

Published online: 4 February 2010

Abstract The chemical bonding aspects of the transition state (TST) of methane activation on a Rh{111} surface are analyzed. Three methods are compared: The *barrier decomposition analysis* of Hu et al. in which the bond between CH is assumed completely broken in the TST (Satterfield, Heterogeneous catalysis in industrial practice, 2nd ed., 1996; Chorkendorff and Niemantsverdriet, Concepts of modern catalysis and kinetics, 2003; Somorjai, Introduction to surface chemistry and catalysis, 1994); the *activation strain model* of Bickelhaupt in which the CH bond is assumed to be equal to the gasphase CH interaction energy (Christmann, Surface science reports, 1988; Nørskov and Christensen, Science, 2006; Forsberg, Chemical engineering progress, 2005); and a model in which the interaction energies between CH, and of the H atom and CH_3 with the catalyst are all given *equal* attention, the *symmetric transition state analysis*. This symmetric transition state analysis would *not* yield a result different from the traditional methods if all bonds were additive and decoupled. But, as our results show, that is not in general the case. The position of the maximum in non-additivity can be considered a descriptor for the position of the TST on the reaction coordinate. At the TST, we find that the three interactions are of comparable strength.

B. S. Bunnik · G.-J. Kramer · R. van Santen (✉)
Schuit Institute of Catalysis, Chemical Engineering and Chemistry, Eindhoven Technical University, P.O. Box 513, 5600 MB Eindhoven, The Netherlands
e-mail: R.A.v.Santen@tue.nl

B. S. Bunnik
e-mail: bouke@sg10.chem.tue.nl

G.-J. Kramer
e-mail: G.J.Kramer@tue.nl

Keywords CH_x · Methane activation · Brønsted—Evans—Polanyi relation · Lateness

1 Introduction

In recent years Brønsted—Evans—Polanyi [1, 2], or linear energy, relations have been shown to be valid for several classes of surface catalysis reactions, including the methane activation reaction.

Inspired by the work of Nørskov et al. [3], Michaelides et al. [4] analyse transition state (TST) energies using *barrier decomposition analysis*, decomposing the reaction barrier with respect to the of association reaction into two parts. One part depends on the adsorption energies of the product fragments. The other part is the (repulsive) interaction between those product fragments. On the association path this arises in the pre-TST from which internal molecular bond formation starts, because of sharing of surface atoms. Subsequent papers by Hu et al. [4–6][1] explore in more detail the results of such decompositions for several reactions. The Bickelhaupt [7–9] *activation strain model* also decomposes the methane activation reaction. In the activation strain model, the energy of the CH bond is assumed similar to the gasphase interaction of that structure and relates to changes in the TST energy via the interaction with the reactive complex.

Because of the high value of the Brønsted—Evans—Polanyi proportionality constant for such reactions, it has been suggested that the methane activation transition state is late [10, 11]. However, in our earlier study of methane

[1] In the following text we will use the notation "Hu et al. [4–6]" to mean the *barrier decomposition analysis* and references [4–6] collectively.

activation on Rh{111} we found indications that the transition states are more in between "late" and "early" [12]. Also, earlier work by Ciobîcă et al. [13] on methane activation on Ru0001 supports a similar view. van Santen and Neurock [14, 15] provided a formal quantum-chemical analysis that arrives at the same conclusions.

Here we develop a general way of analyzing TST structures and energies without involving simplifying assumptions. We combine insights from *barrier decomposition analysis* and the *activation strain model* and extend and generalize them.

The starting point of our method of analysis is the insight that reactions such as methane activation are quintessentially 3-body reactions, with the three interacting bodies being the molecular fragments ($A = CH_3$, $B = H$)and the catalyst (C = Rh{111})—in our case the active atoms of the surface; in other cases it might be a reactive complex.

The nature of the (catalytic) reaction is such that a pre-existing bonding scheme (reactant) goes through a transition state where *all* 3 *entities* interact, resulting in a bonding scheme (product) that is different from the initial one.

The central thesis of this paper is that in analyzing the development of bonding strengths over the course of a reaction, one should give *equal* attention to the making and breaking of *all* bonds $\langle AB \rangle$, $\langle AC \rangle$ and $\langle BC \rangle$. This sets our analysis apart from those in the literature, where often only *one* bond is analyzed, chosen on the basis of chemical intuition. We will call this "symmetric transition state analysis".

This symmetric transition state analysis would *not* yield a different result from the traditional method if all bonds were additive and decoupled. But—as will become apparent later, and is intuitively clear at this stage—that is not the case, in general. This non-additivity will be shown to not only have an important effect on the understanding of the bonding scheme, but is also found to be useful as a descriptor for the "lateness" of the transition state.

We show the results of the symmetric transition state analysis on methane activation on Rh{111}, and give an answer to the question of how "late" the transition state for this activation is.

2 Characterization of Transition States ("Early" Versus "Late")

In literature we can find several starting points for characterizing the structure and energy of a transition state. In the next section, we describe two approaches to examine how "late" or "early" a transition state is with respect to the reaction coordinate. One is the *barrier decomposition method* used by Hu et al. [4–6] for explaining activation energy differences. The other analysis is the *activaton strain model* by Bickelhaupt [7–9]. Both decompose the system into parts in an effort to decouple some relevant interaction(s) from the others. Note that these two approaches each focus on a different interaction between parts of the system. Their choice is based on a preconceived idea of what the relevant interaction is.

Before looking into these two approaches, however, we will introduce a schematic framework that will serve to clarify differences and commonalities of the two approaches. Following the subsequent description of the two, this same framework will serve to describe our own, generalized, decomposition analysis.

2.1 Schematic Representation of the System as Consisting of Three Separate Parts

For our purposes, a dissociation or the reverse, association, reaction can be described as a system ABC consisting of three components: (1) a molecular fragment A, (2) a molecular fragment B, and (3) the catalyst C, that have changing geometries and experience three different interactions between them over the reaction. This results in a different bonding scheme for each value of the reaction coordinate. Figures 1, 2 and 3 show a schematic view of several special points during the reaction.

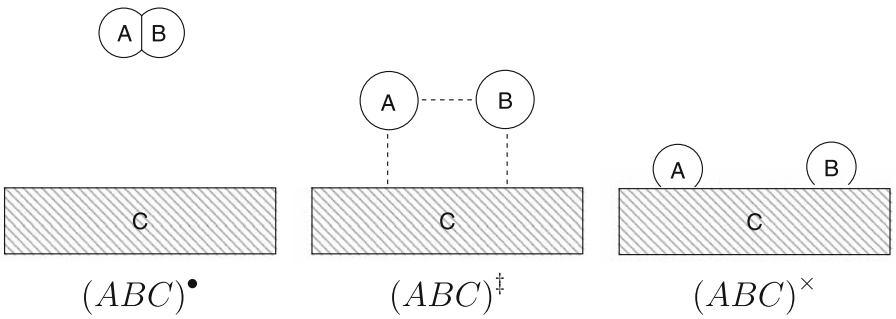

Fig. 1 Schematic representation of the studied association/dissociation system consisting of parts A, B, and C. On the left is shown state "•", where AB is a gas molecule formed from A and B while C is an empty catalyst (surface); we call the energy of this state $E^{\bullet}_{ABC}$. On the right A and B are dissociated onto C in state "×"; this state has energy $E^{\times}_{ABC}$. The middle schematic represents the transition state "‡"; here the bond between A and B is weakened and A and B both have some bonding with C. The energy in the transition state is $E^{\ddagger}_{ABC}$

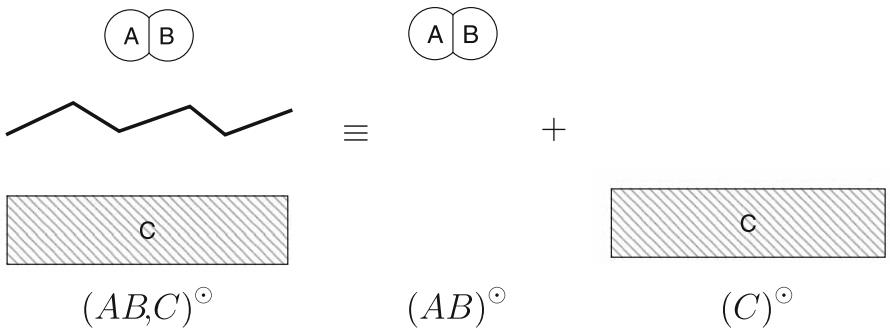

Fig. 2 Schematic representation of the studied association/dissociation system consisting of parts *A*, *B*, and *C*. Reference state used by Bickelhaupt [7–9], "⊙". Gas phase molecule *AB* and catalyst *C* are separate, without interaction between the two parts. Thus, the system can be divided into two independent parts, represented by a zig-zag line separating them. The energy for this state is $E^{\odot}_{ABC} = E^{\odot}_{AB} + E^{\odot}_{C} \equiv E^{\odot}_{AB,C}$

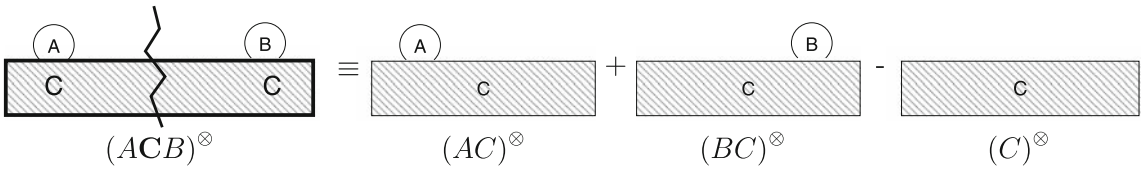

Fig. 3 Schematic representation of the studied association/dissociation system consisting of parts *A*, *B*, and *C*. State used as reference dissociated state by Hu et al. [4–6], "⊗". The two dissociated products *A* and *B* are adsorbed (infinitely) separate on the catalyst *C*, such that the reference state can be treated as the sum of two independent systems, with energy $E^{\otimes}_{ABC} = E^{\otimes}_{AC} + E^{\otimes}_{BC} - E^{\otimes}_{C} \equiv E^{\otimes}_{\mathbf{C}AB}$ (where the $E^{\otimes}_{C}$ preserves the amount of active catalyst sites on both sides of the equation, keeping the mass balance). Note that the "central" component, catalyst *C*, is shown in bold between *A* and *B*, to signify that their bonding is only to that component, not with each other

Figure 1 shows three obviously relevant points along the reaction coordinate, with on the left the associated state "•", at the right the dissociated state "×", and in between the transition state "‡".

In the associated state *A* and *B* are bonded together into a (gasphase) molecule *AB* and *C* is the empty catalyst (surface) with (hardly) any bonding between *AB* and *C*; the system $(ABC)^{\bullet}$ has energy $E^{\bullet}_{ABC}$. In the dissociated state molecule *AB* is dissociated into *A* and *B*. They both are adsorbed onto the catalyst *C*; the energy is $E^{\times}_{ABC}$. In the transition state *A*, *B*, and *C* all (potentially) interact strongly; the energy is $E^{\ddagger}_{ABC}$.

We actually have two more interesting points; a state which we will call "⊙," where molecule *AB* is not bonding to *C* at all (see Fig. 2), so that:

$$E^{\odot}_{ABC} = E^{\odot}_{AB} + E^{\odot}_{C} \equiv E^{\odot}_{AB,C}; \tag{1}$$

and a state "⊗", where *A* and *B* are dissociated and adsorbed but (infinitely) far away from each other, so that they may be seen as two different, independent systems (shown in Fig. 3):

$$E^{\otimes}_{ABC} = E^{\otimes}_{AC} + E^{\otimes}_{BC} - E^{\otimes}_{C} \equiv E^{\otimes}_{\mathbf{C}AB}. \tag{2}$$

The notation for (*A***C***B*) has the "central", shared, component *C* in between *A* and *B*, to indicate that there is only bonding with *C*, but *not between A* and *B*.

Often it is not simple to find the strength of an individual interaction from the energy of the complete system because the bonds interact. Splitting up the system into several parts for which the 2-body interaction(s) *can* be determined and which eliminates interactions between some of the components, reduces the complexity of the systems that have to be calculated. Then, comparing the (sum of the) energies of these less complex 2-body systems with the energy of the full system gives an effective strength of the missing interaction(s).

An important realization is that for this to give real and chemically accurate values for the interaction energies, adding up the three 2-body interaction energies should give the total interaction energy of the full system. If this is the case we can call the interactions "additive", and it means they are not (strongly) coupled. Intuitively, this is not likely exactly true or we would have been able to determine how they influence each other and what the transition state bonding scheme is right away without constructing the full system firt.

We will return to this condition in 5 to check the validity of the approach(es) described in Sects. 2.2 and 2.3. In describing our own "symmetric transition state analysis" (3), we will determine criteria for checking this condition as well. In 4 we will check how well it holds for the first step of methane activation.

2.2 Decomposing Reaction Barriers

Michaelides et al. [4] find that linear energy relations can be observed for a large group of reactions and identify three distinct classes of reactions, of which classes I: CH-cleavage in molecular fragments; and II: Diatomic activation (as in CO) and cleavage of CH bonds in adsorbed species, show a similar slope, but a very different offset, and thus very different reaction barriers.

To the authors, the slopes of the energy curves are associated with the Brønsted—Evans—Polanyi parameter α, so that the slope for these classes being close to one indicates that the transition state structure is similar to that of the product state. They thus consider these reactions to be overwhelmingly late in terms of their reaction coordinate.

To understand the existence and behavior of these reaction classes, Michaelides et al. turn to the association reaction. This is convenient as the transition state of a late dissociation reaction is expected to be similar to the starting point of the association reaction. Thus, for the association reaction, the activation barrier is thought to be almost independent of the reaction energy, and the adsorption energies.

Using the schematic view of the system from 2.1, we describe the *barrier decomposition analysis* approach of Hu et al. [4–6] as being built up of two overlapping combinations of A, B, and C in their TST condition "‡" (middle panel of Fig. 1) and "⊗" (Fig. 3). That state is the reference used by the barrier decompoition analysis in studying the association reaction. Because the transition states are all thought to be late, they should correspond to the adsorption of the two adsorbates, without bonding between them.

The reaction barrier $E^{\ddagger|\otimes}_{ABC}$ [2] is decomposed as follows:

$$E^{\ddagger|\otimes}_{ABC} = {}^{\ddagger|\otimes}_{A\mathbf{C}B} + \epsilon^{\ddagger}_{A\mathbf{C}B}, \tag{3}$$

where $E^{\ddagger|\otimes}_{ABC}$ is the activation energy with respect to the two (infinitely) separated dissociated states (i.e. reference ⊗), while ${}^{\ddagger|\otimes}_{A\mathbf{C}B}$ is mostly the energy required to bring each of the two adsorbates into their transition state position from this reference state. The difference between ${}^{\ddagger|\otimes}_{A\mathbf{C}B}$ and $E^{\ddagger|\otimes}_{ABC}$ is $\epsilon^{\ddagger}_{A\mathbf{C}B}$. It is used as a quantitative measure for the (repulsive) interactions between co-adsorbates at transition states.

The three components of Eq. 3 are shown in Fig. 4. The corresponding energies are:

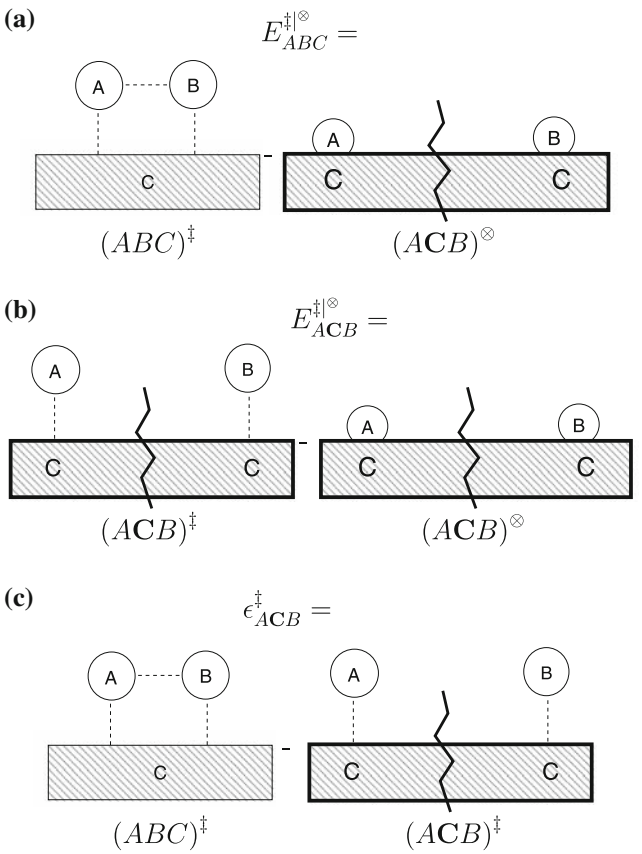

Fig. 4 Schematic depiction of components and energies used by Hu et al. [4–6]. **a** $E^{\ddagger|\otimes}_{ABC}$ is the difference between the transition state energy and the energy of the dissociated state "⊗": $E^{\ddagger|\otimes}_{ABC} = E^{\ddagger}_{ABC} - E^{\otimes}_{ABC} \equiv E^{\ddagger}_{ABC} - E^{\otimes}_{A\mathbf{C}B}$. **b** ${}^{\ddagger|\otimes}_{A\mathbf{C}B}$ is the energy of bringing each of the two association reactants into their transition state condition from their separately dissociated states: ${}^{\ddagger|\otimes}_{A\mathbf{C}B} = E^{\ddagger}_{A\mathbf{C}B} - E^{\otimes}_{A\mathbf{C}B}$. **c** $\epsilon^{\ddagger}_{A\mathbf{C}B}$ is the difference between the energy of the transition state and the energy of the two individual association reactants in their transition state condition: $\epsilon^{\ddagger}_{A\mathbf{C}B} = E^{\ddagger}_{ABC} - E^{\ddagger}_{A\mathbf{C}B}$

$$E^{\ddagger|\otimes}_{ABC} = E^{\ddagger}_{ABC} - E_{A\mathbf{C}B}\otimes$$
$${}^{\ddagger|\otimes}_{A\mathbf{C}B} = E_{A\mathbf{C}B}\ddagger - E_{A\mathbf{C}B}\otimes$$

filling in these two into Eq. 3 we find:

$$\epsilon^{\ddagger}_{A\mathbf{C}B} = E^{\ddagger}_{ABC} - E^{\ddagger}_{AC} - E^{\ddagger}_{BC}, \tag{4}$$

obtaining $\epsilon^{\ddagger}_{A\mathbf{C}B}$. Now, we immediately see that $\epsilon^{\ddagger}_{A\mathbf{C}B}$ is the change in interaction due to bringing the two reactants, already in their respective TST conditions, together in the transition state. This energy combines direct interaction between A and B (presumably small, as this is a late dissociation transition state) and a repulsive interaction due to bonding competition of A and B with C.

Michaelides et al. [4] determine that the difference between their class I and II is that $\epsilon^{\ddagger}_{A\mathbf{C}B}$ is much larger for

[2] We use a notation derived from 2.1 here; The translation to the notation used by Hu et al. [4–6] in their *barrier decomposition analysis* is: $E^{\text{ass}}_{a} \mapsto E^{\ddagger|\otimes}_{ABC}$; $E_{\text{trans}} \mapsto {}^{\ddagger|\otimes}_{A\mathbf{C}B}$; and $E_{\text{int}} \mapsto \epsilon^{\ddagger}_{A\mathbf{C}B}$.

class II reactions because A and B share bonding to a surface atom in the transition state; $E^{\ddagger|\otimes}_{\mathbf{A}C\mathbf{B}}$, related to the changes in adsorption energies of A and B for different catalysts, is small for these classes.

Liu and Hu [5], Liu et al. [6] find a need to refine the above for hydrogenation reactions, splitting up $\epsilon^{\ddagger}_{\mathbf{A}C\mathbf{B}}$ to determine the effects of bonding compensation and Pauli repulsion, showing a linear relation between the valency of the dehydrogenated species and Pauli repulsion. This results in a relation of the reaction barrier with the valency of the decomposition products.

So, while the barrier decomposition analysis used by Hu et al. [4–6] works, Liu and Hu, Liu et al. divide $\epsilon^{\ddagger}_{\mathbf{A}C\mathbf{B}}$ further to explain their results. Depending on the reaction studied, the relevant decomposition may differ.

2.3 Following Components of System-Energy During a Reaction Step

In their study on stabilization of the transition state due to interaction with a reactive complex, following the energy changes over the reaction of a dissociating methane molecule in contact with a Pd atom, de Jong and Bickelhaupt [7–9] have a different way to decompose the TST than described in the above section; they use the *activation strain model* of chemical reactivity.

We can describe the decomposition and analysis using the notation from 2.1, just like we did for the barrier decomposition analysis in 2.2. The activation strain model uses the gas phase AB and lone reactive complex C as reference ("$\odot$", shown in Fig. 2 for the transition state). In this approach all three situations shown in Fig. 1, and intermediate positions of the reaction coordinate are subject to analysis.

In the activation strain model, $E^{|\odot}_{ABC}$[3], the energy with respect to the reference, is:

$$E^{|\odot}_{ABC} = E^{|\odot}_{AB,C} + \epsilon_{AB,C}, \tag{5}$$

with $E^{|\odot}_{AB,C}$ the energy change of the dissociating molecule in the gas phase. This energy is equal to the energy needed for deformation of the methane geometry during this reaction (w.r.t. reference "$\odot$"). Here, $\epsilon_{AB,C}$ is the interaction with the reactive complex. The TST energy $E^{\ddagger|\odot}_{ABC}$ is the dissociation barrier.

Although Fig. 5 shows the parameters of Eq. 5 only in the transition state, the equations are equivalent for the other conditions, except for the reaction coordinate. We find that $E^{|\odot}_{AB,C}$ is:

[3] Here too, we use a notation derived from 2. 1; The translation to the notation used for the *activation strain model* by Bickelhaupt [7–9] is: $\Delta E \mapsto E^{|\odot}_{ABC}$; $\Delta E_{\text{strain}} \mapsto E^{|\odot}_{AB,C}$; and $\Delta E_{\text{int}} \mapsto \epsilon_{AB,C}$. Note that we dropped the Δ as the energies are always with respect to the reference state.

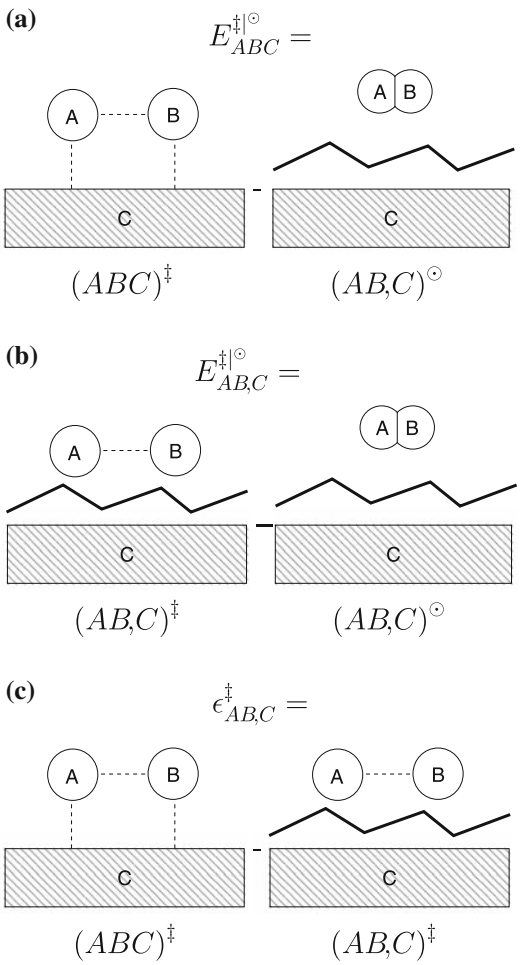

Fig. 5 Schematic depiction of components and energies used by Bickelhaupt [7–9] **a** $E^{\ddagger|\odot}_{ABC}$ is the difference between the transition state energy and the gas phase reference "$\odot$" (Fig. 2): $E^{\ddagger|\odot}_{ABC} = E^{\ddagger} = E^{\ddagger}_{ABC} - E^{\odot}_{ABC} \equiv E^{\ddagger}_{ABC} - E^{\odot}_{AB,C}$. **b** $E^{|\odot}_{AB,C}d$ is the energy needed to deform the gas phase reactant AB into the transition state condition from the reference state "$\odot$". $E^{|\odot}_{AB,C}d = E^{\ddagger}_{AB,C} - E^{\odot}_{AB,C}$. **c** $\epsilon^{\ddagger}_{AB,C}$ is the difference between the energy of the transition state and the dissociation reactant AB in the transition state condition $\epsilon^{\ddagger}_{AB,C} = E^{\ddagger}_{ABC} - E^{\ddagger}_{AB,C}$

$$E^{|\odot}_{AB,C} = E^{\ddagger}_{AB,C} - E^{\odot}_{AB,C}$$

and Fig. 5a shows that $E^{|\odot}_{AB,C}$ is the cost of straining the A–B bond, bringing AB into the transition state condition. We can determine $\epsilon_{AB,C}$, the interaction with the reactive complex, by realizing that:

$$\begin{aligned} E^{|\odot}_{ABC} &= E_{ABC} - E^{\odot}_{ABC} \\ &\equiv E_{ABC} - E^{\odot}_{AB,C}; \end{aligned}$$

Figure 5b shows the transition state situation, with energy $E^{\ddagger|\odot}_{ABC}$. Filling in Eq. 5 gives the result that:

$$\epsilon^{\ddagger}_{AB,C} = E^{\ddagger}_{ABC} - E^{\ddagger}_{AB,C}. \tag{6}$$

This situation is shown in Fig. 5c. Here, the interaction that is studied is the effective adsorption energy of the molecule AB onto the reactive complex C. More generally, $\epsilon_{AB,C}$ is the adsorption interaction of A and B with the catalyst.

The sum of the A and B adsorption energies in the product state is the same as $\epsilon_{AB,C}$ if those energies are with respect to the gas phase reference $(AB, C)^{\odot}$. For methane dissociative adsorption, most numbers in literature are with respect to this reference.

As might be expected, de Jong and Bickelhaupt find that $E^{|\odot}_{AB,C}$ increases monotonically with the reaction coordinate as the bond is broken. The expected behavior of $\epsilon_{AB,C}$ is a different one. It could be expected to increase as molecule AB approaches the reactive complex, while closer to the dissociated state, $\epsilon_{AB,C}$ usually becomes negative as the interaction with that reactive complex increases and the A–B bond weakens. Interestingly, de Jong and Bickelhaupt find that $\epsilon_{AB,C}$ *decreases* monotonically, indicating that there is is no barrier for the (deformed) methane molecule to approach the reactive complex. This means that the reaction barrier is *only* caused by destabilization of the adsorbate as it deforms.

It follows that the transition state position along the reaction coordinate depends on the relative strength of the interaction with the Pd atom, but can be decoupled from the methane adsorption energy. This matches with the late transition states that Hu et al. [4–6] find for such reactions, with $\epsilon_{AB,C}$ decreasing stronger than $E^{|\odot}_{AB,C}$ increases. For an early transition state, there would be a region close to the start of the reaction where $\epsilon_{AB,C}$ would be (strongly) positive. de Jong and Bickelhaupt do find that the strength of the A–B bond is still quite considerable at the transition state, though.

2.4 Comparing the Two Transition State Decomposition Approaches

The two approaches described earlier in this section show us different aspects of a transition state, observing the reaction from different viewpoints. Both approaches have in common that they decompose the transition state and then focus on one of the interactions present to explain energetics and kinetics of the reaction.

The full system has a multi-body interaction from which we cannot easily find the strength of the separate interactions, and thus the two approaches calculate simpler 2-body subsystems that incorporate only part of the interactions in the system, while the remaining interactions follow from the difference with the full system.

Knowing their transition states to be (very) late, Hu et al. [4–6] concentrate on comparing the differences between the dissociated state and the transition state, taking the strength of the adsorbate–surface bond as a given. They separate the placement and deformation of the adsorbates into the transition state, $E^{\ddagger|\otimes}_{\mathbf{ACB}}$, from the interaction between them $(\epsilon^{\ddagger}_{\mathbf{ACB}})$. Because the transition state is late, inter-adsorbate bonding should be negligible, making $\epsilon^{\ddagger}_{\mathbf{ACB}}$ close to zero or positive (due to strong bond competition and Pauli repulsion).

The activation strain model instead looks at the energy remaining in the (deforming) methane, $E^{|\odot}_{AB,C}$, comparing that to the reactant state. Their $\epsilon_{AB,C}$ is the sum of adsorbate–catalyst interactions, including any bonding of the adsorbate(s) to the reactive complex, but also bonding competition and Pauli repulsion. Their $E^{|\odot}_{AB,C}$ contains the bonding between the two adsorbates, but it also includes deformation of the adsorbates into their TST geometries.

While the two approaches do not exactly provide the same information, $E^{|\odot}_{AB,C}$ and $\epsilon^{\ddagger}_{\mathbf{ACB}}$ are close to being each others inverse and $\epsilon_{AB,C}$ is almost the inverse of $E^{\ddagger|\otimes}_{\mathbf{ACB}}$. The different references only shift the energies but don't change their relations.

To sum up, the two approaches are quite similar in approach. And, although they make different choices of what is relevant, they provide similar information. Both choices of what is relevant are made on reasonable grounds, but the Hu et al. [4–6] decomposition is a bit more complicated. It is quite possible that yet another decomposition could have been made on other reasonable grounds.

The activation strain work introduces a nice extra by following changes in energy of the different components along the reaction coordinate. This can easily be done for the Hu et al. [4–6] approach as well, lifting its restriction to late transition states.

2.5 Total Interaction Energy of the System

If the two pairs of energies would be exactly inverse, taking them together should be close to the total bonding between the components. The total bonding can be separately determined from E_{ABC} and the sum of the energy of the separate components (see Fig. 6):

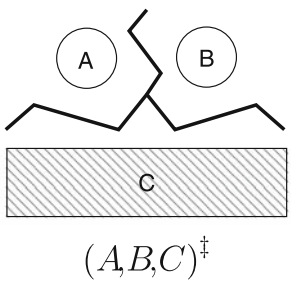

Fig. 6 Schematic representation of the studied association/dissociation system consisting of A, B, and C. This is our atomic reference, with no interaction between the three parts. The energy is thus the sum of the "internal" energies of the three. The energy difference between this state and that of the full system (Fig. 1) is equal to the interaction between the three parts

$$\sum_{i}^{A,B,C} E_i = E_{A,B,C}. \tag{7}$$

$E_{A,B,C}$ includes the individual deformation of the three components, eliminating a difference between $\epsilon^{\ddagger}_{A\mathbf{C}B}R$ and $E^{|\odot}_{A,B,C}$. We can compare the resulting total bonding from the two decompositions to this value, to get an idea of how "additive" the interactions are.

2.6 Validity of the Two Transition State Decomposition Analyses

The two decomposition methods so far described in essence assume that the interactions in the TST are additive and can be accurately described using 2-body interactions.

The Bickelhaupt [7–9] *activation strain model* decomposes the TST energy into the gasphase energy of the strained molecular fragment, corrected for by the interaction of the strained molecule with the reactive complex.

The Hu et al. [4–6] *barrier decomposition analysis* instead views the interaction of the reaction products with the metal. surface as so strong that the intra-reactant can be considered completely broken. The product side of the reaction is now the reference state.

In the following we propose an alternative analysis that allows determination of the non-additive energy terms. We illustrate this method by analysis of the first step of methane activation on Rh111.

3 Symmetric Transition State Analysis

For a system that can be divided into three individual components, such as the methane activation, there are three interactions between the components, and thus three equivalent decompositions which deal with those three interactions in turn, complementing each other.

We use the notation developed in the previous section to describe the two pairs of three complementary decompositions. Starting with the more intuitive set of decompositions derived from the activation strain model by Bickelhaupt, we not only have system AB,C but also the complementary AC,B and BC,A. We can obtain energies equivalent to $\epsilon_{AB,C}$ (Fig. 5) for the effective value of the two missing interactions as shown in Fig. 7; we call this method 1.

The three complementary barrier decomposition analysis-like decompositions are, in addition to the $A\mathbf{C}B$ one described already (see 2.2), $B\mathbf{A}C$ and $C\mathbf{B}A$. Figure 8 illustrates the notation used for these two decompositions, and shows that they are indeed complementary to $A\mathbf{C}B$ (compare Fig. 3). Figure 9 shows how the effective energy of the one missing interaction is derived from this set of complementary decompositions; we call this method 2.

As a reminder, the one "central" component is shown bold in these diagrams, to signify that it appears in two of the separate 2-body subsystems that form these systems.

It is not a coincidence that for each row of the three systems, the central component of Fig. 9 is the one that does not have bonding in Fig. 7. Each row in the two figures shows the decompositions that give information on the same interaction. Figure 7 gives the energy of the studied interaction in the absence of other bonding; Fig. 9 gives the energy remaining to be accounted for after taking the two other bonds into account.

As noted in 2.5, we can compare the interaction energies we obtain from these decompositions with the state where we have no interaction between the three components of the system (shown in Fig. 6). The difference between the full system and state AB,C is the lack of interactions between the three parts A, B, and C. The difference in energy, $\epsilon_{A,B,C}$, is:

$$\epsilon_{A,B,C} = E_{ABC} - E_{A,B,C} \equiv E_{\langle ABC\rangle} \tag{8}$$

$$\epsilon_{A,B,C} \overset{\text{additive}}{\mapsto} E_{\langle AB\rangle} + E_{\langle CA\rangle} + E_{\langle BC\rangle}, \tag{9}$$

where the $E_{\langle ABC\rangle}$ notation refers to the interaction *between* A, B and C, but does not include their internal energies as those are already contained in $E_{A,B,C}$. Equation 9 holds when the interactions are "additive", so that interactions can be split up as done there.

The sum of the three different energies found from Fig. 7 is:

$$\begin{aligned} &\epsilon_{AB,C} + \epsilon_{AC,B} + \epsilon_{BC,A} \\ &\overset{eqns.(1,6,7)}{=} 3 \times E_{ABC} - E_{AB} - E_{AC} - E_{BC} - E_{A,B,C}. \end{aligned} \tag{10}$$

We can rewrite the subsystem energies as:

$$E_{AB} = E_{\langle AB\rangle} + E_A + E_B.$$

Using that together with Eq. 7 in Eq. 10, then applying Eq. 8 and subtracting $\epsilon_{A,B,C}$ from the result, we obtain the combined interaction energy $\epsilon_{\sum_1}$:

$$\epsilon_{\sum_1} \equiv 2 \times \epsilon_{A,B,C} - E_{\langle AB\rangle} - E_{\langle AC\rangle} - E_{\langle BC\rangle},$$

and if the interactions are "additive", we can Use Eq. 9:

$$\overset{\text{additive}}{=} 2 \times \epsilon_{A,B,C} - \epsilon_{A,B,C} = \epsilon_{A,B,C}. \tag{11}$$

We can now check how "additive" the interactions are by comparing their sum (minus one $\epsilon_{A,B,C}$) with $\epsilon_{A,B,C}$:

$$\epsilon_{\sum_1} : \begin{cases} \epsilon_{\sum_1} \approx \epsilon_{A,B,C} & \text{''additive'' interactions,} \\ \epsilon_{\sum_1} < \epsilon_{A,B,C} & \text{''non-additive'', amplified, interactions,} \\ \epsilon_{\sum_1} > \epsilon_{A,B,C} & \text{''non-additive'', weakened, interactions.} \end{cases} \tag{12}$$

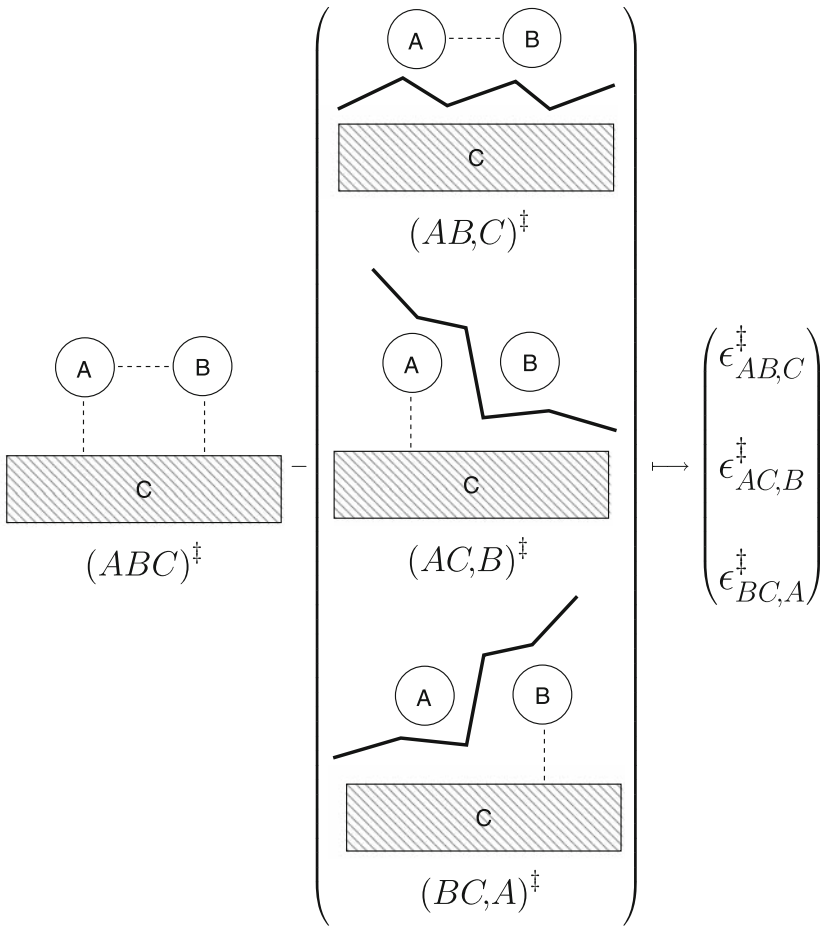

Fig. 7 Schematic representation of symmetric transition state analysis of an association/dissociation system consisting of parts *A*, *B*, and *C*, shown for the transition state. This is a set of decompositions that are physically equivalent to the one used by Bickelhaupt [7–9] (see Fig. 5); we will refer to this as method 1. There are three different interactions to be studied. The top system has on the left the full system, and on the right only $\langle AB \rangle$. The differences are the effective *A*–*C* and *B*–*C* interactions. The second and third equations on the right contain the complementary systems to the one on the first row; they deal with $\langle AC \rangle$ and $\langle BC \rangle$, respectively

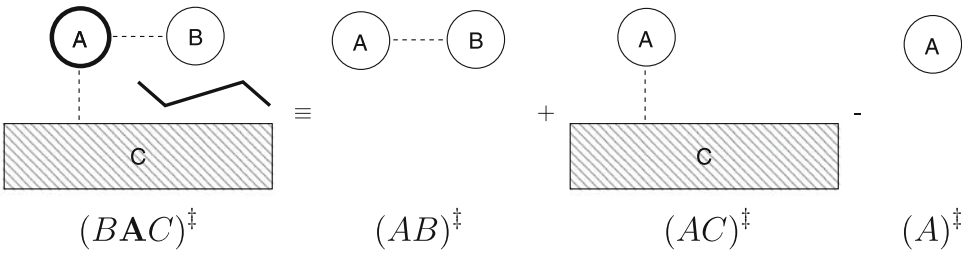

Fig. 8 In Fig. 9, the notation shown here on the left is used as a shorthand for the system composed out of the elements shown on the right. This is fully equivalent to the notation used in Fig. 3, and similar to the way the zig-zag line was used in Fig. 2

If $\epsilon_{\sum_1}$ is about equal to $\epsilon_{A,B,C}$ that means the set of 2-body interactions perfectly model the interactions in the full system; but if $\epsilon_{\sum_1}$ is considerably more or considerably less negative then $\epsilon_{A,B,C}$ that means that in the real system, the interactions are weakened, respectively increased, compared to the 2-body interactions. We will use Eq. 12 in Sect. 4 when we apply the analysis developed here to methane activation.

Equation 11 confirms the complementary nature of the systems in Fig. 7, each giving information about part of the system, but together providing a more complete view of the interactions in the full system, especially when related to the total total interaction energy in that full system.

A similar equation can be set up for the set of systems from method 2 in Fig. 9, giving:

$$\epsilon_{\sum_2} \equiv \epsilon_{A\mathbf{C}B} + \epsilon_{C\mathbf{B}A} + \epsilon_{B\mathbf{A}C} = \epsilon_{A,B,C}. \tag{13}$$

And Eq. 12 also applies to this sum.

So far, we have developed an analysis that gives us the strength of the interaction energies for each of the interactions in the system, provided they are almost additive, and not influencing each other strongly. We also have a check on how well this condition is met.

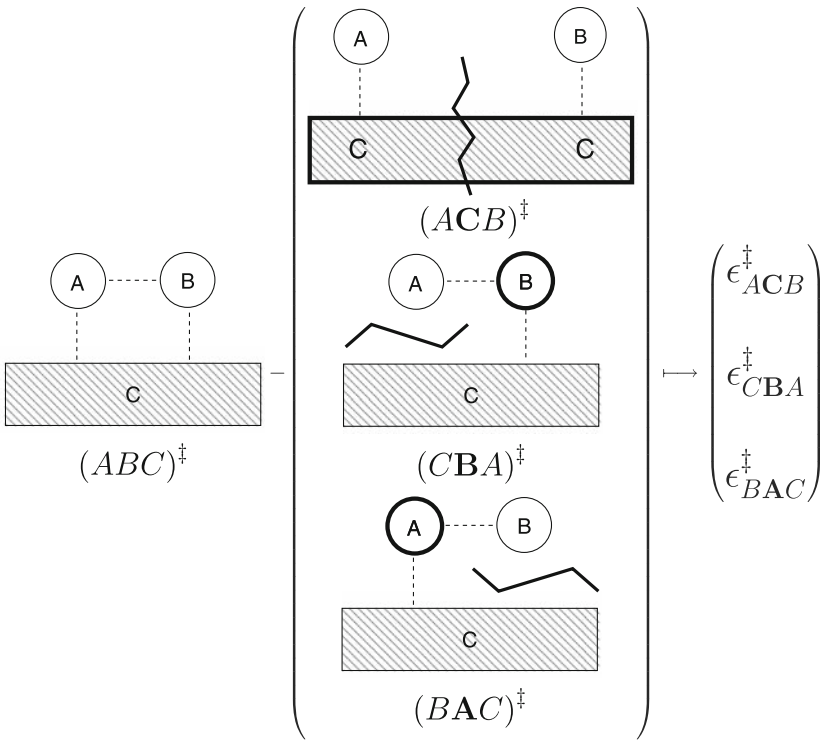

Fig. 9 Schematic representation of symmetric transition state analysis of an association/dissociation system consisting of parts *A*, *B*, and *C*, shown for the transition state. This set of decompositions is physically equivalent to what Hu et al. [4–6] use in their analysis (see Fig. 4; we will refer to this as method 2. There are three different interactions to be studied. The top system has on the left the full system, and on the right $\langle AC\rangle$ and $\langle BC\rangle$, so that the difference is the effective *A*–*B* interaction. The second and third equations on the right contain the complementary systems to the one on the first row; they deal with the interaction of *A* with *C* and of *B* with *C*, respectively

However, even if the interactions are not meeting this condition of being additive, we still obtain some valuable information about the strength of the interactions. Here, we are helped by having the two sets of values for the interaction energies. One of them, the simpler set of method 1, gives an *upper bound* for the interactions, not weakened by the influence of other interactions. The other set, from method 2, gives a *lower bound* of what remains to be accounted for after subtracting the two other 2-body interactions.

Thus, at the least we can always obtain the relative strengths of the three interactions, and how strongly they might be influenced by interactions *between* the bonds.

4 Symmetric Transition State Analysis—An Example

Now that we have a method to study transition states and classify the strength of the interactions between relevant components of the system, it is time to do so. We look at the methane activation reaction on Rh{111} to see how well the approach works.

4.1 Methane Activation on Rh{111}

We reuse results and configurations from the minimum energy path (MEP) determined from our earlier work on methane dissociative adsorption on Rh{111} [12]. For the computational details we refer to Bunnik and Kramer [12] as we used essentially the same setup. The current results follow from single-point (DFT) electronic structure calculations based on the set of configurations that we used to approximate the MEP.

The reaction starts from gas phase methane and goes, via a transition state that has the CH_3–H adsorbed approximately on the "atop" adsorption site, to CH_3(hcp) and H(fcc) co-adsorbed on the met al. surface, and finishes with CH_3 and H adsorbed (infinitely) separate. Figure 10 shows the transition state. The product side is 8.7 kJ mol^{-1} endothermic with respect to the reactant (gas phase

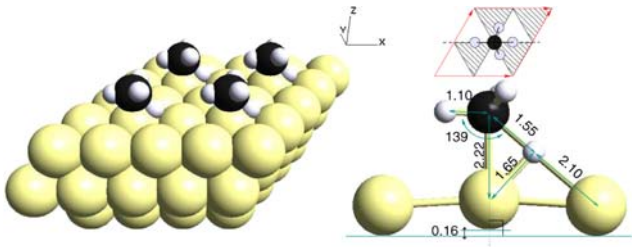

Fig. 10 Transition state for $CH_4 \rightarrow CH_3^* + H^*$. The activated C atom is almost exactly above a surface atom, with the activated C–H bond aligned along a bridge to the next Rh atom. The left panel gives an overview of the surface structure of the fragment. The top right panel is a schematic top-view of the surface unit cell, showing the hexagonal shape, with Rh atoms at the corner of each triangle (shaded: hcp, white: fcc). The dotted line shows the intersection used for the bottom right panel, where several relevant distances (Å) and angles (°) are given

methane and an empty Rh{111} surface), and the CH_3(hcp), H(fcc) co-adsorption is 20.3 kJ mol^{-1} endothermic [12].

In our earlier work we concluded based on geometry (bond lengths), that this transition state was relatively early when compared to some of the other CH_x activation steps:

$$\frac{d^{\ddagger}_{C-H} - d^{\odot}_{C-H}}{d^{\otimes}_{C-H} - d^{\odot}_{C-H}} = \frac{1.69 - 1.10}{2.50 - 1.10} \times 100\% = 42\%, \qquad (14)$$

however, this assumes a clear relation between C–H bond length and energy [12], and even then it is not an absolute measure, depending on the lateness of those other transition states. Still, our results did not indicate a very late transition state such as found by Hu et al. [4–6]. Since we focussed on the CH_3–H part of the system, our approach was more in line with what de Jong and Bickelhaupt do, and we essentially found, similar to that article, that in the transition state, the C–H bond was still quite strong.

4.2 Symmetric Transition State Analysis of Methane Activation

The first step in our symmetric transition state analysis is to decompose the system into the three components CH_3 (A), H (B), and a slab of Rh{111} (C). The sum of the energies of the three components is $E_{A,B,C}$, and the difference with the full system's energy (E_{ABC}) is $\epsilon_{A,B,C}$ (see Eq. 8), which will vary over the reaction. In this case, because the reaction is almost thermodynamically neutral, $\epsilon_{A,B,C}$ is almost equal at the start and end of the reaction, but we are interested in the changes around the transition state, as that shows the difference with E_{ABC}.

Applying the analysis from Sect. 3, specifically, the results from the diagrams in Figs. 7 and 9, we obtain two sets of energy curves, showing the development of the three energies during the reaction. Because set 1 is more intuitively understandable, we first look at the results of this set and will then describe the set 2 briefly in paragraph 4.2.2, in so far as they give additional information.

4.2.1 Results from Method 1

Figure 11 consists of three panels. The bottom panel shows the (development over the reaction of) distances between the three components, allowing a reconstruction of the reaction path. We can divide the reaction in three stages:

1. Approach of methane to the catalyst; A–C and B–C strongly decrease, as does AB–C, while the A–B distance remains unchanged.
2. Transition state region; B–C has a dip; A–B increases strongly at the start of this region.

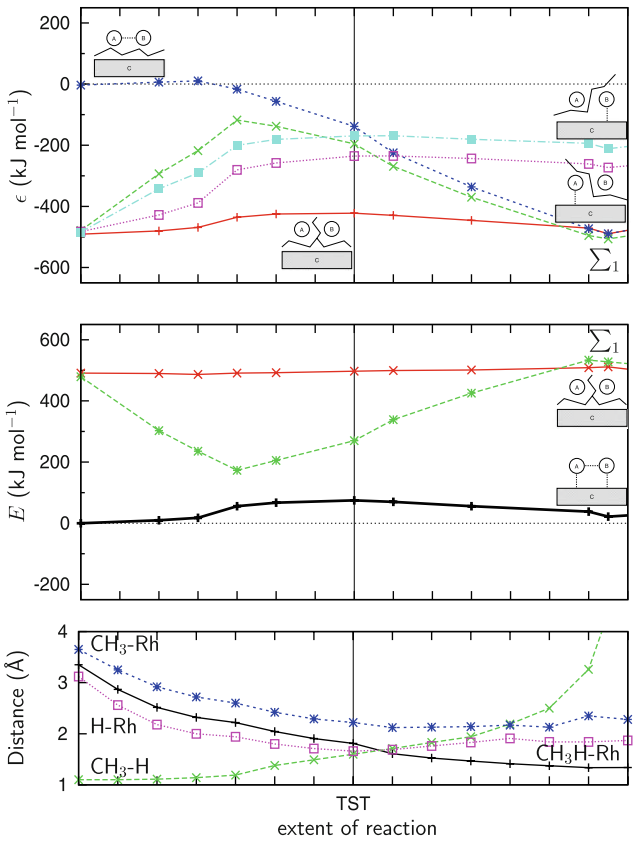

Fig. 11 Symmetric transition state analysis of the activation of CH_4(g) via the transition state to CH_3(hcp) + H(fcc), ending with CH_3 and H adsorbed separately on the Rh{111} surface; method 1. Bottom panel: development of distances between the three components, A: CH_3, B: H and C:Rh{111}, during the reaction step (in Å). The middle and top panel use the notation developed in the previous section to describe the curves they display: ABC: full system; A, B, C : gas phase CH_3, H, and Rh{111}; AB, C : CH_3 –H and Rh{111}; AC, B : CH_3 –Rh{111}, gas phase H; BC, A : H–Rh{111}, gas phase CH_3; and $\sum_1$: sum of those three decompositions (see Eq. 11). Middle panel: energy of ABC and A, B, C and $\sum_1$; Top panel: effective interaction energies derived from Fig. 7

3. The product side; The A–B distance increases strongly while the other distances remain more or less the same.

The middle panel shows the energy for the complete system, E_{ABC} (bottom line) and $E_{A,B,C}$ (upper, red, line). We reuse the schematic pictures from Sect. 3 to indicate which curve is which system. The behavior of the system energy is as follows:

1. E_{ABC} is constant without interaction between the surface and the molecule.
2. E_{ABC} has a maximum (the transition state) and then slopes downward.
3. E_{ABC} slopes downwards, with a somewhat larger step at the end, going down to the energies of the infinitely separately desorbed CH_3 and H.

$E_{A,B,C}$, the internal energy of the components, is almost the same at both ends of the reaction (491 and 511 kJ mol^{-1}, respectively). In addition, it remains almost constant over the whole reaction, only slightly increasing from start to end.

The top panel shows the effective interaction energies ε from Fig. 7. In agreement with $E_{A,B,C}$ being almost constant, the total interaction between the three components, the bottom (red) curve in the panel, is relatively constant (422−490 kJ mol^{-1}), mostly mirroring the shape of the E_{ABC}-curve.

The three remaining solid curves in the panel are the three complementary energies $\varepsilon_{AB,C}$, $\varepsilon_{AC,B}$ and $\epsilon_{BC,A}$. They show the same three stages of the reaction as seen before:

1. $\epsilon_{AB,C}$ remains close to zero, indicating that the C–H bond is still at full strength. This is in agreement with the bond length being unchanged. In contrast, as the distance between methane and the surface decreases, $\epsilon_{AC,B}$ and $\epsilon_{BC,A}$ increase strongly, possibly exponentially. This is helped by the availability of electrons, which, in the full system, were tied up in the bond between CH_3 and H.
2. As the bond length grows, $\epsilon_{AB,C}$ drops somewhat abruptly and steeply down, although it does not go down all the way to $\epsilon_{A,B,C}$ yet. Meanwhile, $\epsilon_{AC,B}$ and $\epsilon_{BC,A}$ reach a value close to their final value, the CH_3 and H adsorption energies, then closely follow the changes in $\epsilon_{A,B,C}$.
3. $\epsilon_{AB,C}$ drops down until it remains close to $\epsilon_{A,B,C}$ at the final two points where CH_3 and H are too far apart to experience bonding. $\epsilon_{AC,B}$ and $\epsilon_{BC,A}$ follow $\epsilon_{A,B,C}$, again mirroring the downwards slope of E_{ABC} in this region.

Note that at the transition state, this curve is less stable then the final system by only 140 kJ mol^{-1}, with the final value of ~490 kJ mol^{-1} still far away. The bond is thus still considerably strong.

As a side note, we can conclude that using bond length to determine the strength of this reaction, as we did earlier, is a reasonable approach, as there is a roughly linear relation between the *A*–*B* bond length and the gas phase bonding strength. However, it is obviously no better then only looking at one of the three interactions.

The (green) $\sum_1$ curves in the top and middle panels is the sum of the three complementary systems (see Eq. 11 and the discussion there). For additive interactions these curves would follow the *A*, *B*, *C* curves, however, the actual behavior is as follows:

1. $\epsilon_{\sum_1}$ rises together with $\epsilon_{AC,B}$ and $\epsilon_{BC,A}$.
2. The rise of $\epsilon_{\sum_1}$ stops at a maximum of "non-additiveness", at the point where $\epsilon_{AB,C}$ starts its decline, following this curve, while the other two ε curves reach their maximum, before the transition state.
3. $\epsilon_{\sum_1}$ follows the further decline of $\epsilon_{AB,C}$ towards $\epsilon_{A,B,C}$.

4.2.2 *Results from Method 2*

Differences between Figs. 7 and 12 are mainly found in the top panel. This panel shows the same (red) $\epsilon_{A,B,C}$ curve, and three complementary ε curves, as well as the sum of those three in the (green) $\epsilon_{\sum_2}$ curve.

Just like in Fig. 11, $\epsilon_{\sum_2}$ begins the 1st stage of the reaction following $\epsilon_{A,B,C}$. In the 2nd stage $\epsilon_{\sum_2}$ rises steeply towards the maximum just before the transition state, where the interactions are the least additive. It then drops

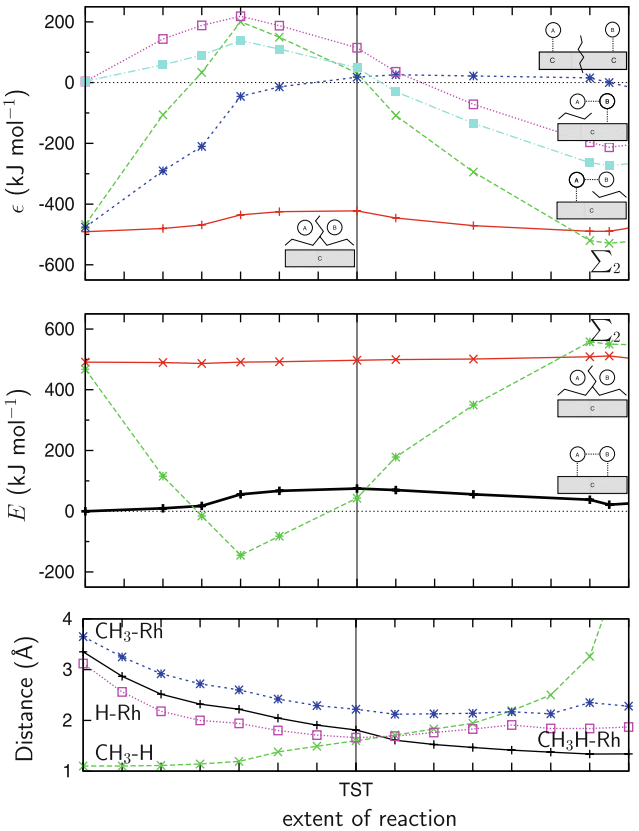

Fig. 12 Symmetric transition state analysis of the activation of CH_4(g) via the transition state to CH_3(hcp) + H(fcc), ending with CH_3 and H adsorbed separately on the Rh{111} surface; method 2. Bottom panel: development of distances between the three components, *A*:CH_3, *B*: H and *C*:Rh{111}, during the reaction step (in Å). The middle and top panel use the notation developed in the previous section to describe the curves they display: *ABC*: full system; *A*, *B*, *C* : gas phase CH_3, H, and Rh{111}; *ACB*: CH_3−Rh{111}-H (see Fig. 3); *BAC*: H-CH_3−Rh{111} (see Fig. 8); *CBA*: CH_3−H−Rh{111}; and $\sum_2$: sum of the those three decompositions (Eq. 13). Middle panel: energy of *ABC* and *A*, *B*, *C* and $\sum_2$; Top panel: effective interaction energies derived from Fig. 9

sharply, and again finds $\epsilon_{A,B,C}$ during the 3rd stage of the reaction. However, in this figure, $\epsilon_{\sum^2}$ clearly shows that calculating the three bonds separately overestimates them, making this composite system about 200 kJ mol^{-1} *more* stable then the original full system.

Reflecting the composite behavior of the used decompositions, the curves for $\varepsilon_{C\mathbf{BA}}$ and $\varepsilon_{B\mathbf{AC}}$ start at zero, but then rise sharply and have a 2nd stage that contains a maximum at the same point as $\epsilon_{\sum^2}$, as they include the full *A–B* interaction and *also* the nearly fully developed *AC* and *BC* interactions, respectively. In the 3rd stage of the reaction their behavior remain a mix between $\epsilon_{AB,C}$ and $\epsilon_{AC,B}$, or $\epsilon_{BC,A}$, respectively. Note that their reactant values are the inverse of the equivalent line in Fig. 11.

The $\varepsilon_{A\mathbf{CB}}$ curve is the sum of the $\epsilon_{AC,B}$ and $\epsilon_{BC,A}$ curves, and because those are almost at their maximum in the transition state, this curve is almost zero from that point on. Looking back from the end towards the transition state, $\epsilon^{\ddagger}_{A\mathbf{CB}}$ increases from zero to about 20 kJ mol^{-1}, which is consistent with the cost of co-adsorption found in our previous work and in literature [12]. This behavior is what reinforced Hu et al. [4–6] in their conclusion of a late transition state, as it seems to confirm that co-adsorption destabilization is the only remaining interaction between CH_3 and H, when seen in isolation without the context of the other interaction.

5 Changes of Bond Orders Over the Reaction

As a check on our results from the symmetric transition state analysis, we calculated bond orders for reactant, TST and product geometries of methane activation.

These bond orders were calculated using simplistic clusters, consisting of the 4 top layer Rh(111) atoms and the CH_3–H adsorbate, derived from our VASP output. For looking at trends in bond orders to confirm other results, as we do here, we believe this to be sufficient. The bond orders follow the definition of Mayer [16], as implemented in the ADF code. Computations have been carried out with the Amsterdam Density Functional program (ADF 2008.01) [17] at the ZORA-BLYP/TZ2P level of relativistic density functional theory: te Velde et al. [18].

Table 1 confirms the behavior of the three bonds that we saw from symmetric transition state analysis, especially in 4.2.1, namely that the C–H bond is weakened in the transition state, but not absent, while the bonds with the met al. surface are already strong in the transition state, but not at their final value yet

At the transition state, the three interactions all have a bond order between 0.3 and 0.6 with the C–Rh{111} bond being the strongest, and the H−Rh{111} bonds being weaker. The C–H bond is at the the lower end of the scale. The different relative strengths concluded from these bond orders as compared to results from the previous section are likely a reflection of the non-additiveness of these bonds. However, the results still indicate that at the transition state the three bonds are all present, and with a strength of the same order.

Note that in the original product state, CH_3 and H bind to three met al. surface atoms, but in our simple cluster, not all those bonds are present. This doesn't influence the transition state, but does show the bonding scheme in the product state to be more similar to the transition state than is the case.

Table 2 shows the bond order of the C–H bond for the *AB, C* system, the only bond present in that system. Comparing the bond order in the transition state with the values from Table 1 clearly shows the tendency of this system to overestimate the strength of the C–H bond during the reaction. Due to interaction with the catalyst, the actual strength of the bond is weaker than the 2-body interaction.

Table 1 Bond orders of the bonds involved in methane activation, C–Rh, C–H^{ts} and H–Rh, at reactant, TST, and product geometries

Bond	Reactant	Transition state	Product
C–H	0.99	0.29	<0.2
C–Rh1	–	0.43	0.54
H–Rh1	–	0.38	0.42
H–Rh2	–	<0.2	0.49

6 Chemical Bonding Analysis of Methane in Its TST

Comparing the 2-body bonding-strengths at the transition state to their maximum values of the gas phase methane C–H bond, or the CH_3 and *H* adsorption energies, we have shown that:

1. The C–H bond is reduced by about 30%, to 350 kJ mol^{-1} out of 490 kJ mol^{-1};
2. The CH_3–Rh{111} is formed for 80%, at 170 kJ mol^{-1} out of 213 kJ mol^{-1};
3. The H-Rh{111} is formed for 86%, at 235 kJ mol^{-1} out of 273 kJ mol^{-1}; and that
4. All three interactions are of comparable strength, between 170 kJ mol^{-1} and 350 kJ mol^{-1}.

Table 2 Bond orders of a methane fragment, calculated at the geometries of reactant, TST and product, in gasphase (i.e. for system *AB, C*, see 2.3)

Bond	Reactant	Transition state	Product
C–H	0.99	0.94	0.89[a]

[a] Overestimated bond-order due to limitations of the calculation

Bond orders confirm that the transition state still has a considerable strength in the C–H bond, even though it is reduced by a bit more than half of the original value.

Non-additivity is a very considerable factor, especially in the most interesting region, around the transition state. In that region, assuming additiveness leads to an overestimation of the interaction strength by up to 333 kJ mol^{-1}, almost 45% of the total bonding interaction. It is due to competition for, and interaction of, electrons in the *full* three-body system.

The 2-body bonding-strengths at the transition state, 350, 170, and 235 kJ mol^{-1}, add up to 755 kJ mol^{-1}. If these are *normalized* to the actual transition state "interaction energy" (422 kJ mol^{-1}), then the interactions are 196, 119, and 132 kJ mol^{-1}, respectively. These are all about half of the full bonding strength of the individual bonds (40%, 56%, 48%).

Both the different ordering of bond strengths seen from bond orders, and the considerably higher bond order calculated for the 2-body C–H bond are due to this effect, and they confirm that it is a large and important aspect, which needs to be taken into account when analyzing a bonding scheme.

In our analysis, we have found that if there is a single descriptor of the 3-body character of the reaction, it is the non-additivity. The location of the transition state with respect to the maximum in non-additivity is a suitable descriptor for the position of the the transition state on the reaction coordinate. For an early reaction we would expect it to occur while the dissociating bond weakens before the surface bonds start forming, while for a very late transition state, the surface bonds would be already fully formed, leaving only little electron density left in the intra-adsorbate bond.

In summary, our symmetric transition state analysis provides a new perspective on the analysis of molecular interactions during a reaction. The advantage of the symmetrical analysis—giving equal emphasis to all three 2-body interactions—avoids drawing conclusions that are biased by *a priori* chemical intuition.

7 Conclusions

Faced with an apparent discrepancy between our work on methane activation on Rh{111} providing evidence for non-"late" transition states, and literature on the "lateness" of transition states for methane activation claiming a universal lateness for such reactions, we developed a new method to analyze transition states.

We compared two different approaches, the *barrier decomposition analysis* by Hu et al. [4–6] and the *activation strain model* by Bickelhaupt [7–9] to study the activation of molecules adsorbed to a catalyst using computational chemistry. These analyses start from different premises on the relative strength of relevant chemical bonds. Both assume pairwise interactions.

A more general approach follows from the realization that in the transition state we are still dealing with a three-body system with three interactions between the individual components that all change in strength and nature during a reaction step. These bonds essentially interact in a quantum-chemical way and hence may have significant delocalization character. This implies that they can be non-additive.

We have analyzed the three-body system of reacting species to determine the non-additive component as a function of reaction coordinate. For this analysis, we decompose the system in three complementary systems, each determining one of three interactions in absence of the others. We follow the development of these three complementary systems over the reaction step. This then gives a ranking of the strength of the three interactions relative to each other. We call this approach "*symmetric transition state analysis*" to stress the importance of the equal treatment of all interactions.

Using the symmetric transition state analysis, it can be made clear that in general the three interactions are coupled and thus "non-additive". Adding up the three 2-body energies thus gives a different result than the interaction in the original system, in general overestimating the strength of those interactions. Only at the start and end, where the interactions can be easily determined from stable state calculations, are they additive.

Not surprising, the interactions are least additive in the transition state region. While at first this seems to indicate that there is only a limited quantitative use for the obtained ranking of interactions, upon further inspection, the amount of non-additiveness itself does give some very interesting information.

We find that the minimum in additivity lies at the point where we have a change from an early stage with a dominating C–H bond to a later stage where adsorption of CH_3 and H to the metal surface are predominant. Seen in this light, the fact that the transition state lies slightly beyond that point leads one to the interpretation that the transition state is more late inclined than early.

Acknowledgements This study is partly sponsored by the Dutch Stichting Technische Wetenschappen (STW, project UPC.5037). We are grateful to M. Bickelhaupt for discussions on his *activation strain model* and thank him for providing us with the bond orders calculations.

References

1. Brønsted J (1928) Chem Rev 5:231
2. Evans M, Polanyi M (1938) Trans Faraday Soc 34:11
3. Nørskov JK, Bligaard T, Logadottir A, Bahn S, Hansen LB, Bollinger PM, Bengaard HS, Hammer B, Sljivancanin Z, Mavrikakis M, Xu Y, Dahl P, Jacobsen CJH (2002) J Catal 209:275
4. Michaelides A, Liu Z-P, Zhang CJ, Alavi A, King DA, Hu P (2003) J Am Chem Soc 125:3704
5. Liu Z-P, Hu P (2003) J Am Chem Soc 125:1958
6. Liu Z-P, Hu P, Lee M-H (2003) J Chem Phys 119:6282
7. Bickelhaupt FM (1999) J Comput Chem 20:114
8. de Jong GT, Bickelhaupt FM (2007) Chem Phys Chem 8:1170
9. van Zeist W-J, Visser R, Bickelhaupt FM (2009) Chem Eur J 15:6112 (Communication)
10. Hammond GS (1955) J Am Chem Soc 77:334
11. Leffler JE (1953) Science, New Series 117:340
12. Bunnik BS, Kramer G-J (2006) J Catal 242:309
13. Ciobîcă IM, Kramer G-J, Ge Q, Neurock M, van Santen RA (2002) J Catal 212:136
14. van Santen RA, Neurock M (2007) Russ J Phys Chem B 1:261
15. van Santen RA, Neurock M (2008) In: Ertl G, Knözinger H, Schüth F, Weitkamp J (eds) Handbook of heterogeneous catalysis, vol. 3. Wiley-VCM, Weinheim, p 1415
16. Mayer I (1983) Chem Phys Lett 97:270
17. ADF: Amsterdam density functional software for chemists Scientific Computing & Modelling NV (SCM)
18. te Velde G, Bickelhaupt FM, Baerends EJ, Fonesca Guerra C, van Gisbergen SJA, Snijders JG, Ziegler T (2001) J Comput Chem 22:931